International Journal of General Medicine

Dovepress

open access to scientific and medical research

Open Access Full Text Article

ORIGINAL RESEARCH

Computed Tomography Morphological Classification of Lung Adenocarcinoma and Its Correlation with Epidermal Growth Factor Receptor Mutation Status: A Report of 1075 Cases

Qi Li[1]
Xiao-Qun He[1,*]
Xiao Fan[2]
Tian-You Luo[1]
Ji-Wen Huo[1]
Xing-Tao Huang[3,*]

[1]Department of Radiology, The First Affiliated Hospital of Chongqing Medical University, Chongqing, 400016, People's Republic of China; [2]Department of Radiology, Children's Hospital of Chongqing Medical University, Chongqing, 400014, People's Republic of China; [3]Department of Radiology, University of Chinese Academy of Sciences Chongqing Renji Hospital (Fifth People's Hospital of Chongqing), Chongqing, 400062, People's Republic of China

*These authors contributed equally to this work

Background: Many delayed diagnoses of lung adenocarcinoma (LADC) are identified due to poor understanding of protean imaging findings. Moreover, clarifying the relationship between computed tomography (CT) morphological classification and epidermal growth factor receptor (EGFR) mutations of LADC might inform therapeutic decision-making while obtaining pathological specimens is difficult. Here, we retrospectively analyzed CT manifestations of LADC and investigated the morphological classification of tumors in relation to EGFR mutation status.

Methods: We included 1075 LADC patients undergoing chest CT and EGFR genotype examinations from January 2013 to January 2019. CT morphological characteristics of tumors were carefully evaluated and their correlation with EGFR mutation status was analyzed using the chi-squared test.

Results: Tumors were divided into eight types: I (peripheral solid nodule/mass; 526/1075, 48.93%), II (central solid nodule/mass; 220/1075, 20.47%), III (subsolid nodule/mass; 92/1075, 8.56%), IV (focal consolidation; 32/1075, 2.98%), V (cystic airspace; 14/1075, 1.30%), VI (multiple lesions with similar appearances to I–V; 85/1075, 7.91%), VII (diffuse consolidation; 53/1075, 4.93%), VIII (occult lesion usually obscured by nonobstructive atelectasis; 53/1075, 4.93%). Type III and IV tumors were more frequent in patients with EGFR mutation, whereas type II and VII tumors were more common in patients without EGFR mutation (all $P < 0.05$). However, we did not identify any significant associations between other tumor types and EGFR mutation status (all $P > 0.05$). Among patients with type VI tumors, EGFR mutation status was closely related to tumor density (all $P < 0.05$). Furthermore, type VII tumors were associated with 19 deletion mutation positive and non-L858R mutation positive (all $P < 0.05$).

Conclusion: LADC can be categorized into eight types based on CT imaging. Improving our understanding of the morphological classification and correlation with EGFR mutation status may contribute to the accurate diagnosis of LADC, while suggesting the presence of underlying EGFR genetic mutations.

Keywords: lung adenocarcinoma, morphology, computed tomography, epidermal growth factor receptor, mutation

Correspondence: Xiao-Qun He
Tel +86 18324179667
Email 18324179667@163.com

Xing-Tao Huang
Department of Radiology, University of Chinese Academy of Sciences Chongqing Renji Hospital (Fifth People's Hospital of Chongqing), No. 24 Renji Road, Nan'an District, Chongqing, 400062, People's Republic of China
Tel +86 13896573793
Fax +86 23 68811487
Email hxt89011721@163.com

Introduction

Lung cancer is a major cause of cancer death globally, with lung adenocarcinoma (LADC) being the most common histological subtype.[1] This subtype exhibits various manifestations on computed tomography (CT), many of which

Received: 21 April 2021
Accepted: 21 June 2021
Published: 21 July 2021

mimic non-malignant processes and often overlap with other diseases.[2] In clinical practice, we have identified a large number of missed or delayed diagnoses of LADC, which is mainly attributable to the lack of knowledge regarding the protean imaging findings associated with this condition. In addition, we have also noticed some unusual CT findings in cases of LADC, which have not yet been well documented. Therefore, it is clear that a comprehensive understanding of the morphological features of LADC based on CT appearance is vital for the prevention of diagnostic errors.

The rapid development of novel targeted therapies has led to increasing integration of genetic analysis with the diagnosis and treatment of LADC, including analysis of epidermal growth factor receptor (EGFR) mutations, Kirsten rat sarcoma viral oncogene homolog mutations, anaplastic lymphoma kinase rearrangement, etc.[3,4] Among these, EGFR is a key receptor of tyrosine kinase, and considerable research has demonstrated that initial therapy with a tyrosine kinase inhibitor instead of standard chemotherapy has a high success rate for patients with advanced lung cancer and EGFR mutations, with reduced complications and toxicity reported.[5,6] Therefore, it is important to evaluate the possibility of EGFR mutation in patients with lung cancer in order to determine appropriate clinical management. Biopsy and sequence testing are routinely used to analyze EGFR genotype; however, detection of mutations is not always possible because obtaining histologic samples is challenging, especially in unresectable or advanced tumors. Currently, CT is the preferred imaging modality for diagnosing lung cancer and evaluating responses to treatment, and the identification of a relationship between CT morphological features and EGFR mutations in the context of LADC may inform therapeutic decision-making in cases where obtaining pathologic specimens is difficult.

To our knowledge, some particular CT features of LADC as well as the correlation between CT morphological classification and EGFR mutation status have not yet been fully clarified. The present study aimed to investigate the CT manifestations and morphological classification of LADC in relation to EGFR mutations.

Materials and Methods

Patients

This retrospective study was conducted in accordance with the Declaration of Helsinki, and used anonymous data and had no potential risks to patients. All its protocols were approved by the ethics committee of The First Affiliated Hospital of Chongqing Medical University, and the need for informed consent was waived due to the retrospective nature. From January 2013 to January 2019, we enrolled all consecutive patients with pathologically diagnosed LADC who underwent chest CT and EGFR genotype examinations at our hospital for which pretherapeutic CT data were stored in our picture archiving and communication system (PACS) and detection results of EGFR genotype were available. Exclusion criteria were as follows: 1) patients with a history of chemotherapy, radiotherapy, or other oncological therapy before CT and EGFR genotype examinations, 2) interval between CT imaging and subsequent surgery, biopsy or cytology, and molecular analysis of EGFR mutation status was over 1 month,[7] and 3) patients with multifocal pulmonary neoplasm in whom not all tumors underwent genetic testing, but some tumors were tested and were negative for EGFR mutation. Moreover, clinical data including age, sex, smoking history, clinical cancer stage, and diagnostic methods were collected.

Epidermal Growth Factor Receptor Mutation Analysis

Surgical specimens, biopsy specimens, and hydrothorax fallen cells of tumors were used for molecular analysis. The EGFR mutation status (exons 18–21) was examined using a real-time polymerase chain reaction-based amplification refractory mutation system with the Human EGFR Gene Mutations Detection Kit (AmoyDx, Xiamen, China). For patients with multifocal lesions, the patient was considered positive for EGFR mutation when at least one lesion was found to be positive for EGFR mutation. Patients were considered negative for EGFR mutation when all lesions were confirmed to be negative for EGFR mutation.

CT Protocols

Chest CT examinations were performed using the Discovery CT750HD (GE Healthcare), Light speed VCT (GE Healthcare), or Somatom Definition Flash (Siemens Healthcare) scanner. All patients underwent CT scanning in the supine position at the end of inspiration during a single breath hold. Imaging parameters were as follows: tube voltage, 120 kVp; tube current, 100–250 mA; and scanning slice thickness/interval, 5 mm/5 mm. A total of 786 patients (73.12% of the study population) received contrast-enhanced scanning and were injected with nonionic

iodinated contrast medium (iohexol 300 mg iodine/mL; Omnipaque, GE Healthcare) at a dosage of 1.5 mL/kg of body weight (total volume: 80–110 mL) using a dual-high-pressure injector via the antecubital vein at a flow rate of 3.0 mL/s. This was followed by injection of 50 mL saline solution. The acquisition times in the arterial phase and delayed phase were triggered at 30 and 120 s, respectively, after the start of contrast medium injection.

CT Image Analysis

All images were reconstructed using a section thickness and slice interval of 1.25 and 1.25 mm, respectively, for imaging analysis. Two radiologists (with 15 and 12 years of experience in chest imaging, respectively) blindly and independently interpreted the axial images on a PACS workstation (Vue PACS, Carestream), and any disagreements were resolved by discussion until a consensus was reached. The following data were recorded for each patient: 1) number of lesions (single/multiple); 2) distribution (single lobe/unilateral multiple lobes/bilateral multiple lobes; left upper and lower lobes; right upper, middle, and lower lobes); 3) location (central, involving the segmental or more-proximal bronchi; peripheral, involving the subsegmental or more-distal bronchi); 4) size (longest diameter of a measurable tumor on axial image in the lung window setting with window width, 1600 Hounsfield units; window level, −600 Hounsfield units); 5) shape (round, oval, polygonal [eg, triangular, rectangular, or trapezoidal], or irregular [with an uneven contour that could not be classified as round, oval, or polygonal]); 6) margin (regular, predominantly smooth; irregular, spiculated/lobulated) and border definition (well- or ill-defined [partially or completely]); 7) density (solid, tumor without ground-glass opacity [GGO] characterized by increased lung attenuation through which lung parenchymal structures, such as the pulmonary vessels or bronchial structures, could be observed; subsolid, tumor with GGO, including pure GGO and mixed GGO [GGO admixed with solid opacity]); 8) internal characteristics (air bronchogram, air-filled bronchus within the tumor; airspace, air attenuation within the tumor, including cavity and pseudo-cavity; necrosis, focal area of low attenuation without enhancement). The bronchial leafless tree sign was defined as an air-filled bronchus manifesting as dilatation, stretching (referring to rigidity and elongation of the air-filled bronchus) or squeezing (referring to narrowing of the bronchus); 9) relationship with surrounding structures (vascular convergence sign, convergence of vessels toward the tumor, only analyzed in peripheral tumors; pleural retraction, connection of linear structures between the tumor and pleura; pleural attachment, attachment of the tumor to the pleura and tumor margin obscured by the pleura); 10) other special CT features based on different patterns of the tumors, such as bronchial abnormalities or obstructive changes in central lung cancers, CT angiogram sign and bulging of the interlobar fissure in pneumonia-type lung cancer, and so on; 11) associated findings (lymphadenopathy, hilar, or mediastinal lymph nodes with short-axis diameter >1 cm; intrapulmonary metastasis, nodules in primary tumor lobe or nontumor lobes; lymphangitic carcinomatosis; pleural or pericardial metastasis). The clinical cancer stages were evaluated according to the 8th edition of the American Joint Committee on Cancer staging system for non-small cell lung cancer.[8] After the first interpretation of CT images, the two radiologists decided the morphological classification criterion through discussion. Then, they reviewed all CT images again and classified the tumors.

Statistical Analysis

Statistical analyses were performed by using IBM SPSS Statistics for Windows (version 19.0; IBM Corp., Armonk, NY, USA). Single-sample Kolmogorov–Smirnov analysis was used to test the variance in homogeneity of the measurements. Normally distributed quantitative data are expressed as mean ± standard deviation, and non-normally distributed data are presented as median ± interquartile range. The Chi-squared test was employed to analyze the correlation between morphological classification and EGFR mutation status. Interobserver agreement between the two observers was assessed using Kappa scores. A two-tailed P value of <0.05 was considered to indicate statistical significance.

Results

Observer Reproducibility

The agreement between the two observers was almost perfect with a measured kappa value of 0.983 for the CT morphological classification. Additionally, CT features of tumors were all in good agreement with the kappa values ranging from 0.830 to 1.00.

Clinical Characteristics of the Study Population

A total of 1135 patients were initially included in the present study. Of these, 60 were excluded due to a history of anti-tumor therapy (n = 22), interval between CT imaging and subsequent analysis of over 1 month (n = 15), and negative results for

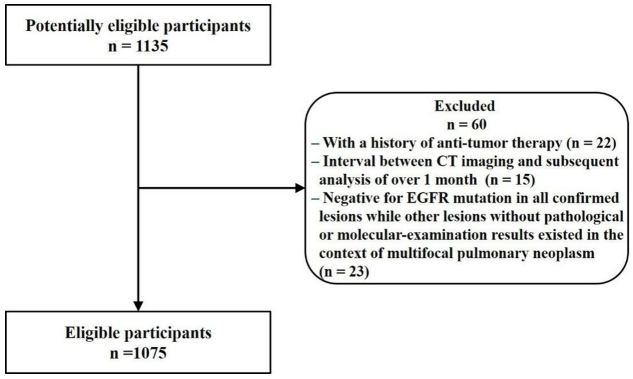

Figure 1 Flow diagram for this study.

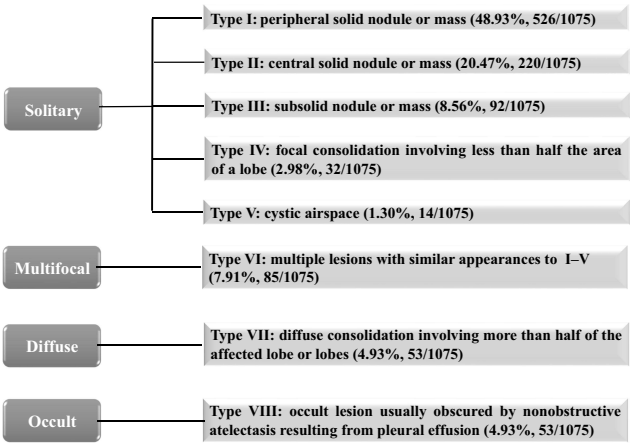

Figure 2 Computed tomography morphological classification of lung adenocarcinoma.

EGFR mutation in all confirmed lesions, whereas other lesions without pathological or molecular examination results existed in the context of multifocal pulmonary neoplasm (n = 23). Finally, 1075 patients with LADC were included for analysis. The flow diagram for this study is shown in Figure 1. The clinical characteristics of the study population are summarized in Table 1.

CT Morphological Classification of Lung Adenocarcinoma

The results of CT morphological classification of LADC are illustrated in Figures 2 and 3. According to the location, shape, density, and number of tumors, eight different patterns were identified. Among them, type I accounted for the majority, followed by II, and then III. Types I–II appeared as a solid nodule, or a mass in the peripheral or central locations (with a round, oval, or irregular contour) (Figure 3A and B). Type III manifested as a subsolid nodule, or a mass (with a round, oval, or irregular contour) (Figure 3C). Types IV and V LADC were associated with some unique findings. Type IV presented as a focal consolidation involving less than half the area of a lobe, usually containing air bronchogram (with a polygonal [eg, triangular, rectangular, or trapezoidal] contour) (Figure 3D); Type V appeared as a solitary thin-walled cystic airspace (Figure 3E and F). Type VI was characterized by multifocal lesions, which shared similar appearances to I–V (Figure 3G and H). Type VII presented as diffuse consolidation involving more than half of the affected lobe or lobes, usually accompanied by multiple nodules or GGO (Figure 3I). Type VIII tumors were occult and usually obscured by nonobstructive atelectasis resulting from pleural effusion (Figure 3J). The presence of tumors was confirmed by follow-up CT or positron emission tomography-computed tomography (PET/CT) scanning (Figure 3K).

Table 1 Clinical Characteristics of the Study Population

Characteristics	Number (%)
Age (years)	
Median ± interquartile range	62 ± 15
Range	24–89
Sex	
Male	592/1075 (55.07)
Female	483/1075 (44.93)
Smoking	
Nonsmokers	578/1075 (53.77)
Smokers	497/1075 (46.23)
Clinical cancer stage	
Stage I	192/1075 (17.86)
Stage II	54/1075 (5.02)
Stage III	153/1075 (14.23)
Stage IV	676/1075 (62.88)
Method of diagnosis	
Surgery resection	346/1075 (32.19)
Percutaneous biopsy	261/1075 (24.28)
Bronchoscopic biopsy	276/1075 (25.67)
Cytology	192/1075 (17.86)

Notes: Data are presented as number/total (%) unless otherwise stated.

CT Characteristics of Lung Adenocarcinoma in Relation to Morphological Classification

Table 2 shows the representative CT features of LADC types I–VIII. Among the 884 patients with type I–V LADC, 849 lesions involved a single lobe and 35 involved multiple lobes. For the former, the upper lobe was the most common location (503/849, 59.25%), followed by

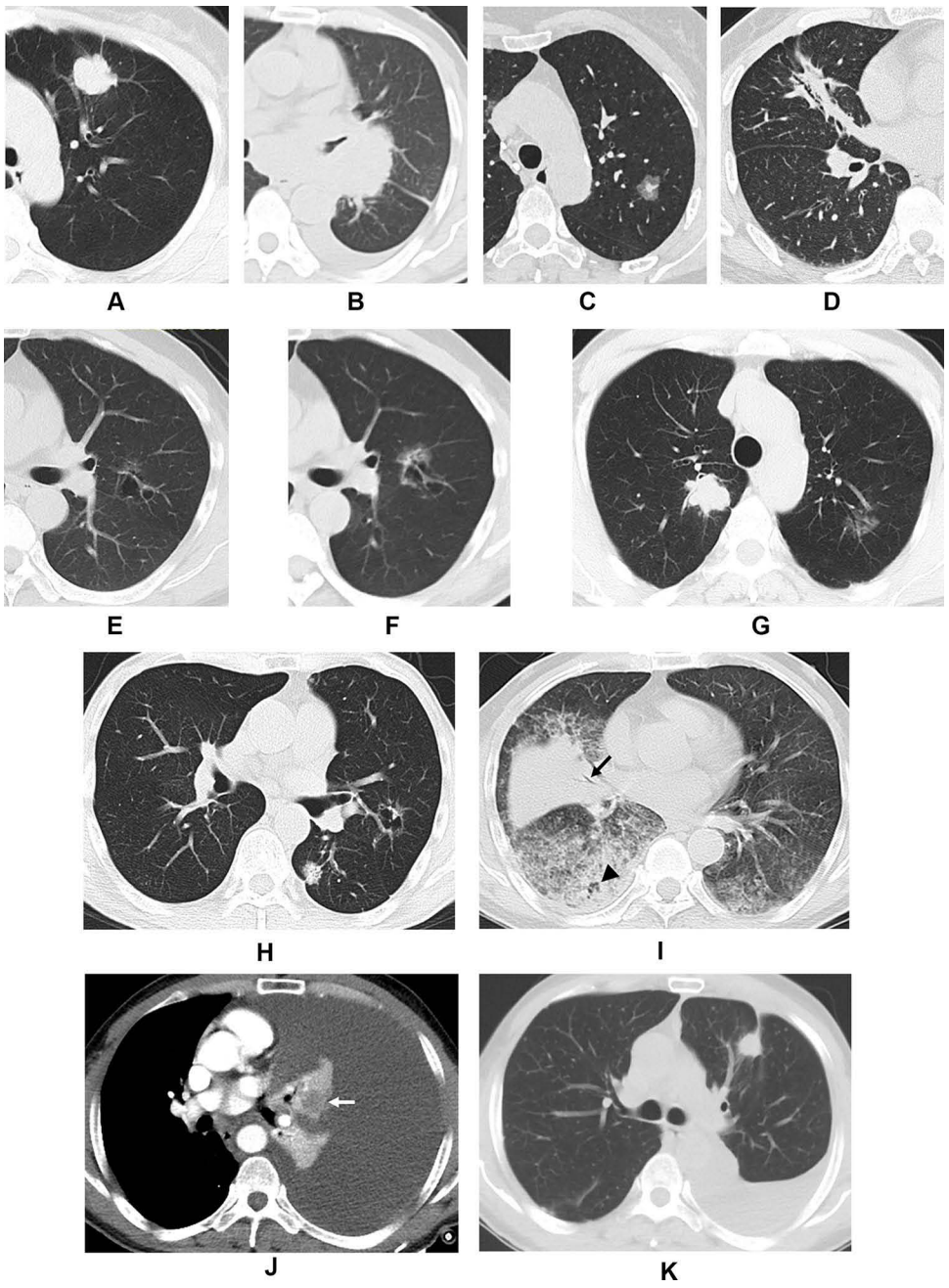

Figure 3 Computed tomography images demonstrating the morphological classification of lung adenocarcinoma. Representative axial images of (**A**) Type I, showing a peripheral solid nodule with lobulation and pleural retraction in the left upper lobe; (**B**) Type II, showing a central solid mass in the left hilum with bronchiostenosis of the left upper lobe; (**C**) Type III, showing a subsolid nodule with irregular margin in the left upper lobe; (**D**) Type IV, showing focal triangular consolidation with bronchial leafless tree sign and pleural retraction in the right middle lobe; (**E**) Type V, showing a cystic airspace with irregular margins, septation, nonuniform cyst wall, and ground-glass opacity in the left upper lobe; (**F**) second image of (**E**) taken 45 months later showing an increase in lesion size with thickening of the cyst wall and increased ground-glass opacity; (**G**) Type VI in a 60-year-old male showing a solid nodule in the right upper lobe and a subsolid nodule in the left upper lobe which were surgically confirmed as adenocarcinoma; (**H**) Type VI in a 75-year-old male showing a solid nodule and a cystic airspace in the left lung which were surgically confirmed as adenocarcinoma; (**I**) Type VII, showing multiple consolidations and ground-glass opacity in both lungs with deadwood-like air bronchogram (black arrow) and air space (black arrowhead); (**J**) Type VIII, showing left massive pleural effusion with atelectasis in which the tumor was embedded, resulting in heterogeneous enhancement (white arrow), adenocarcinoma cells were found by cytological examination of the hydrothorax; (**K**) Follow-up imaging of (**J**) revealed the presence of a solid nodule (ie, a tumor) in the left upper lobe with partial absorption of the hydrothorax after two cycles of chemotherapy.

the lower upper lobe (284/849, 33.45%), then the right middle lobe (62/849, 7.30%). The median size of tumors was 2.80 ± 1.92 cm (range: 0.60–9.50 cm). In type I, irregular margins (particularly lobulation), pleural retraction, and attachment were frequently detected. Among the 220 patients with type II, 186 lesions were well defined

Table 2 Computed Tomography Characteristics of Lung Adenocarcinoma with Type I–VIII Features

Classification	CT Characteristics	Number (%)	Location	Number (%)
I (n = 526)	Irregular margins	510/526 (96.96)	RUL	157/526 (29.85)
	Air bronchogram	56/526 (10.65)	RML	37/526 (7.03)
	Air space	81/526 (15.40)	RLL	99/526 (18.82)
	Necrosis*	78/403 (19.35)	LUL	148/526 (28.14)
	Vascular convergence sign	142/526 (27.00)	LLL	80/526 (15.21)
	Pleural retraction	306/526 (58.17)	RMLs	2/526 (0.38)
	Pleural attachment	255/526 (48.48)	LMLs	3/526 (0.57)
II (n = 220)	Irregular margins**	184/186 (98.92)	RUL	54/220 (24.55)
	Bronchial stenosis or occlusion	211/220 (95.91)	RML	19/220 (8.64)
	Bronchial obstructive changes	161/220 (73.18)	RLL	33/220 (15.00)
	Obstructive emphysema	12/161 (7.45)	LUL	53/220 (24.09)
	Obstructive pneumonia	102/161 (63.35)	LLL	31/220 (14.09)
	Obstructive atelectasis	87/161 (54.04)	RMLs	21/220 (9.55)
	Obstructive bronchiectasis	20/161 (12.42)	LMLs	9/220 (4.09)
III (n = 92)	Irregular margins	82/92 (89.13)	RUL	31/92 (33.70)
	Air bronchogram	26/92 (28.26)	RML	3/92 (3.26)
	Air space	32/92 (34.78)	RLL	13/92 (14.13)
	Vascular convergence sign	28/92 (30.43)	LUL	33/92 (35.87)
	Pleural retraction	52/92 (56.52)	LLL	12/92 (13.04)
	Pleural attachment	17/92 (18.48)		
IV (n = 32)	Air bronchogram	29/32 (90.63)	RUL	11/32 (34.38)
	Bronchial leafless tree sign	22/32 (68.75)	RML	2/32 (6.25)
	Air space	12/32 (37.50)	RLL	7/32 (21.88)
	GGO within or around the consolidation	25/32 (78.13)	LUL	8/32 (25.00)
	Pleural retraction	28/32 (87.50)	LLL	4/32 (12.50)
	Pleural attachment	9/32 (28.13)		
V (n = 14)	Irregular margins	12/14 (85.71)	RUL	3/14 (21.43)
	Nonuniform cyst wall	13/14 (92.86)	RML	1/14 (7.14)
	Septation in cyst	12/14 (85.71)	RLL	2/14 (14.29)
	Wall nodule	9/14 (64.29)	LUL	5/14 (35.71)
	GGO around the cyst	10/14 (71.43)	LLL	3/14 (21.43)
	Pleural retraction	6/14 (42.86)		
	Pleural attachment	4/14 (28.57)		
VI (n = 85)	All lesions presenting as I and/or II (solid)	17/85 (20.00)	Single lobe	10/85 (11.76)
	All lesions presenting as III (subsolid)	21/85 (24.71)	RMLs	12/85 (14.12)
	I or II + III (solid + subsolid)	31/85 (36.47)	LMLs	5/85 (5.88)
	I and/or III + IV and/or V (mixed)	16/85 (18.82)	BMLs	58/85 (68.24)
VII (n = 53)	Bronchial leafless tree sign	39/53 (73.58)	Single lobe	9/53 (16.98)
	Air space	27/53 (50.94)	RMLs	9/53 (16.98)
	Bulging of the interlobar fissure	28/53 (52.38)	LMLs	1/53 (1.89)
	CT angiogram sign***	16/42 (38.10)	BMLs	34/53 (64.15)
	Multiple nodules	36/53 (67.92)		
	GGO	49/53 (92.45)		
	Lymphadenopathy	41/53 (77.36)		
VIII (n = 53)	Atelectasis with heterogeneous enhancement	48/53 (90.57)	Unilateral PE	41/53 (77.36)
	Absence of pleural thickening	17/53 (32.08)	Right	14/41 (34.15)
	Localized irregular pleural thickening	4/53 (7.55)	Left	27/41 (65.85)
	Extensive irregular pleural thickening	21/53 (39.62)	Bilateral PE	12/53 (22.64)
	Extensive linear pleural thickening	11/53 (20.75)	Right-predominant	5/12 (41.67)
	Lymphadenopathy	28/53 (52.83)	Left-predominant	7/12 (58.33)

Notes: Data are presented as number/total (%). *Necrosis was not assessed in 123 patients who did not undergo contrast-enhanced scanning. **Margins were not assessed in 34 patients because of ill-defined border. ***CT angiogram sign was not assessed in 11 patients who did not undergo contrast-enhanced scanning.

Abbreviations: CT, computed tomography; GGO, ground-glass opacity; RUL, right upper lobe; RML, right middle lobe; RLL, right lower lobe; LUL, left upper lobe; LLL, left lower lobe; RMLs, right multiple lobes; LMLs, left multiple lobes; BMLs, bilateral multiple lobes; PE, pleural effusion.

with a median size of 5.00 ± 2.02 cm (range: 1.20–11.00 cm), while 34 were ill-defined. The most common findings included irregular margins, bronchial stenosis or occlusion, and bronchial obstructive changes. Patients with type III were associated with a high frequency of mixed GGO (89/92, 96.74%), with few cases of pure GGO (3/92, 3.26%), and observations such as irregular margins and pleural retraction, which were quite common. Type IV LADC was found to be more likely to exhibit bronchial leafless tree sign, GGO within, or around the consolidation, and pleural retraction, while type V usually presented with irregular margins, nonuniform cyst wall, septation in cyst, wall nodules, and GGO around the lesion.

Among the 85 patients with type VI, 297 lesions (mean: 3.49 lesions per patient, range: 2–22 lesions per patient) were identified with a median size of 2.20 ± 2.30 cm (range: 0.70–12.70 cm), and 206 (mean: 2.42 lesions per patient, range: 1–5 lesions per patient) were pathologically confirmed. This pattern usually manifested as a complicated combination of types I–V. For patients with type VII, diffuse consolidation with bronchial leafless tree sign, airspace, bulging of the interlobar fissure, CT angiogram sign, GGO, multiple nodules, and lymphadenopathy were typical features. For patients with type VIII, most patients (41/53, 77.36%) exhibited unilateral moderate or massive pleural effusion, 14 on the right side and 27 on the left; additionally, a small number of patients (12/53, 22.64%) exhibited bilateral pleural effusion, five with right-predominant and seven with left-predominant effusion. Heterogeneous enhancement of atelectasis due to hydrothorax, irregular thickening of pleura, and lymphadenopathy were characteristic findings.

Correlation Among EGFR Mutation Status, Clinical Features, and Morphological Classification of Lung Adenocarcinoma

We found 566 (52.65%) patients to be positive for EGFR mutation. EGFR mutation rates were significantly higher in females (338/483, 69.98%) than in males (228/592, 38.51%) and in nonsmokers (387/578, 66.96%) than in smokers (179/497, 36.02%) (all $P < 0.001$). The Chi-squared test indicated types II, III, IV, and VII to be associated with EGFR mutation status (all $P < 0.05$). Types III and IV LADC were significantly more frequent in patients with EGFR mutation positive, whereas types II and VII were significantly more common in patients with EGFR mutation negative. However, no significant associations were found between other types and EGFR mutation status (all $P > 0.05$) (Table 3). For patients with type VI, most of them (47/85, 55.29%) were found to be EGFR mutations positive, and EGFR mutation status was correlated with the density of tumors. EGFR mutations rates were significantly higher in patients with subsolid lesions than in those without ($P < 0.001$) and in patients with all lesions presenting as subsolid densities (type III) than in those without ($P < 0.05$), whereas the rate of EGFR mutations was significantly lower in patients with all lesions manifesting as solid densities (type I or II) than in those without ($P < 0.001$; Table 4).

Among the 566 patients with EGFR mutation positive, 40.64% (230/566) harbored a single 19 deletion mutation, 46.82% (265/566) harbored a single L858R mutation, and 12.54% (71/566) harbored other mutation subtypes. Type VII tumors were found to be correlated to 19 deletion mutation positive and non-L858R mutation positive (all $P < 0.05$). However, no significant associations were found between other types of LADC and the mutation status of 19 deletion and L858R (all $P < 0.05$; Table 5).

Discussion

The histological heterogeneity of LADC is well known, and this condition has been classified into various histological subtypes according to the current LADC classification system,[9] each of which exhibits different clinical behaviors. Based on these pathological characteristics, LADC can present with a broad spectrum of CT findings ranging from subsolid to solid densities, and the lesions may be single or multifocal.[10,11] The present study evaluated the imaging features of LADC and identified eight patterns of morphological classification. Familiarity with the overall morphological classification and awareness of the typical CT signs associated with each type will aid clinicians to better diagnose and treat LADC.

Our study reveals type I–III features to be the most common, usually presenting with a typical appearance of lung cancer. Previous studies have shown that the density of the tumors is closely related to the histological subtype of LADC.[9,12,13] LADC with a predominantly solid or micropapillary pattern tends to manifest as a solid lesion, lepidic-predominant LADC is associated with subsolid lesions, and a papillary- or acinar-predominant pattern may present as both solid and subsolid lesions. We found type IV to be characterized by focal consolidation usually with air bronchogram. Air bronchogram is an important

Table 3 Correlation Among Epidermal Growth Factor Receptor Mutation Status of Lung Adenocarcinoma, Clinical Features, and Morphological Classification

Characteristics	Total	EGFR Positive (n = 566)	EGFR Negative (n =509)	*P* value[a]
Sex				
Male	592	228/592 (38.51)	364/592 (61.49)	<0.001
Female	483	338/483 (69.98)	145/483 (30.02)	
Smoking				
Never	578	387/578 (66.96)	191/578 (33.04)	<0.001
Smoker	497	179/497 (36.02)	318/497 (63.98)	
Type I				
Yes	526	284/526 (53.99)	242/526 (46.01)	0.389
No	549	282/549 (51.37)	267/549 (48.63)	
Type II				
Yes	220	101/220 (45.91)	119/220 (54.09)	0.025
No	855	465/855 (54.39)	390/855 (45.61)	
Type III				
Yes	92	60/92 (65.22)	32/92 (34.78)	0.012
No	983	506/983 (51.48)	477/983 (48.52)	
Type IV				
Yes	32	25/32 (78.13)	7/32 (21.88)	0.003
No	1043	541/1043 (51.87)	502/1043 (48.13)	
Type V				
Yes	14	8/14 (57.14)	6/14 (42.86)	0.735
No	1061	558/1061 (52.59)	503/1061 (47.41)	
Type VI				
Yes	85	47/85 (55.29)	38/85 (44.71)	0.611
No	990	519/990 (52.42)	471/990 (47.58)	
Type VII				
Yes	53	19/53 (35.85)	34/53 (64.15)	0.012
No	1022	547/1022 (53.52)	475/1022 (46.48)	
Type VIII				
Yes	53	22/53 (41.51)	31/53 (58.49)	0.096
No	1022	544/1022 (53.23)	478/1022 (46.77)	

Notes: Data are presented as number/total (%). [a]Chi-squared test.
Abbreviation: EGFR, epidermal growth factor receptor.

diagnostic feature of infective consolidation; however, LADC can display features very similar to infection, which may result in diagnostic error. Specific CT findings, such as dead bronchial leafless tree sign, GGO within or around the lesion, and pleural retraction, indicate the possibility of cancer, which should therefore be considered. We found type V to have a particular CT presentation: thin-walled cystic airspace, which may be interpreted by a pulmonary cyst, bleb, or bulla. The mechanism underlying the formation is unclear, although the check-valve mechanism, wherein the tumor originates from the alveolar wall and produces abundant fibrous tissue, causing focal stenosis of the airway and formation of a unidirectional check-valve, has been proposed.[14,15] Tan et al reported morphological features that are indicative of cystic lung cancer including nonuniform cyst walls, septation within the cyst, wall nodules, GGO around the cyst, and irregular margins, which were in agreement with our study.[15] Clinicians should be aware that LADC can present with such signs initially, and lesions can enlarge over time with wall thickening and an increase in solid components.

In the present work, we found the incidence of multifocal LADC (type VI) to be relatively common. Multifocal LADC represents a morphologic description of tumors

Table 4 Correlation Between the Density of Tumors and Epidermal Growth Factor Receptor Mutation Status in Patients with Type VI Morphological Features

Density of Tumors	Total	EGFR Positive (n = 47)	EGFR Negative (n = 38)	*P* value[a]
Containing subsolid nodule or mass				
Yes	65	46/65 (70.77)	19/65 (29.23)	<0.001
No	20	1/20 (5.00)	19/20 (95.00)	
All presenting as subsolid nodule or mass				
Yes	21	18/21 (85.71)	3/21 (14.29)	0.001
No	64	29/64 (45.31)	35/64 (54.69)	
All presenting as solid nodule or mass				
Yes	17	1/17 (5.88)	16/17 (94.12)	<0.001
No	68	46/68 (67.65)	22/68 (32.35)	

Notes: Data are presented as number/total (%). [a]Chi-squared test.
Abbreviation: EGFR, epidermal growth factor receptor.

Table 5 Correlation Between Epidermal Growth Factor Receptor 19 Deletion and L858R Mutation Status and CT Morphological Classification of Lung Adenocarcinoma

Characteristics	Total (n = 566)	19del (+) (n = 230)	Non-19del (+) (n = 336)	*P* value[a]	L858R (+) (n = 265)	Non-L858R (+) (n = 301)	*P* value[a]
Type I							
Yes	284	122/284 (42.96)	162/284 (57.04)	0.259	129/284 (45.42)	155/284 (54.58)	0.504
No	282	108/282 (38.30)	174/282 (61.70)		136/282 (48.23)	146/282 (51.77)	
Type II							
Yes	101	36/101 (35.64)	65/101 (64.36)	0.260	52/101 (51.49)	49/101 (48.51)	0.300
No	465	194/465 (41.72)	271/465 (58.28)		213/465 (45.81)	252/465 (54.19)	
Type III							
Yes	60	25/60 (41.67)	35/60 (58.33)	0.864	30/60 (50.00)	30/60 (50.00)	0.602
No	506	205/506 (40.51)	301/506 (59.49)		235/506 (46.44)	271/506 (53.56)	
Type IV							
Yes	25	10/25 (40.00)	15/25 (60.00)	0.947	12/25 (48.00)	13/25 (52.00)	0.904
No	541	220/541 (40.67)	321/541 (59.33)		253/541 (46.77)	288/541 (53.23)	
Type V							
Yes	8	1/8 (12.50)	7/8 (87.50)	0.204	6/8 (75.00)	2/8 (25.00)	0.207
No	558	229/558 (41.04)	329/558 (58.96)		258/558 (46.24)	300/558 (53.76)	
Type VI							
Yes	47	15/47 (31.91)	32/47 (68.09)	0.204	24/47 (51.06)	23/47 (48.94)	0.543
No	519	215/519 (41.43)	304/519 (58.57)		241/519 (46.44)	278/519 (53.56)	
Type VII							
Yes	19	14/19 (73.68)	5/19 (26.32)	0.003	4/19 (21.05)	15/19 (78.95)	0.022
No	547	216/547 (38.94)	331/547 (60.51)		261/547 (47.71)	286/547 (52.29)	
Type VIII							
Yes	22	7/22 (31.82)	15/22 (68.18)	0.390	7/22 (31.82)	15/22 (68.18)	0.150
No	544	223/544 (40.99)	321/544 (59.01)		258/544 (47.43)	286/544 (52.57)	

Notes: Data are presented as number/total (%). [a]Chi-squared test.

from CT images because differentiating intrapulmonary metastases from a new primary cancer may be difficult, especially when the tumors' histology is similar.[16,17] Our results show that these lesions may be distributed in a number of patterns, although they are more likely to be located in multiple lobes of both lungs. Moreover, tumors were often at different stages from pre-invasive to invasive and therefore the findings varied from type I to V within a single patient. Similarly, type VII is often misdiagnosed as pneumonia, thereby delaying the diagnosis. Given that the CT findings of this type often overlap with those of pneumonia, it is essential to evaluate imaging findings in combination with other clinical data (eg, leukocyte count or efficacy of antibiotic treatment) to make a diagnosis. Type VIII has rarely been reported previously, and this type is the most easily misdiagnosed pattern of LADC due to poor understanding of the CT features. Atelectasis with heterogeneous enhancement, irregular pleural thickening, and lymphadenopathy are highly indicative of malignancy.[18,19] In our opinion, for patients with massive pleural effusion, contrast-enhanced CT scanning is necessary to enable radiologists to differentiate the obscured tumor from the atelectasis. Moreover, PET-CT may be a superior method of detecting tumors of this type.[20,21]

Recently, many radiologists have studied the possibility of obtaining information on gene mutations indirectly from imaging or radiogenomic features of lung cancer.[7,22–28] Liu et al[7] stated that CT imaging features of LADC in combination with clinical variables can be used for the prediction of EGFR mutation status. Tu et al[27] found that the radiomics signature showed better performance for predicting EGFR mutants than all the clinical and morphological features, with an AUC of 0.762 and 0.775, respectively, in a training and validation cohort. However, the lack of standardization of acquisition parameters, inconsistent radiomic methods, and lack of reproducibility are the major limitations of radiogenomic analysis, making its clinical application difficult. As compared with artificial intelligence imaging, CT morphology is more direct and easily obtained for lesion analysis, which has an important practical value. Moreover, most studies have focused on patients with early-stage lung cancer or solitary tumors treated with surgical resection. Minimal research has focused on patients with advanced-stage disease or multiple/diffuse unresectable tumors.[7,22–25] The majority of the population receiving targeted therapy in the present studies had advanced lung cancer. We identified morphological classification to be predictive of EGFR mutation among patients with all stages of LADC and tumors with diverse numbers or distributions. There were several major findings in relation to this: First, we found EGFR mutation to be associated with the female sex and non-smoking status, which supports previous studies.[7,22–25] Second, we found types III and IV to be more frequent among patients with EGFR mutation positive, whereas types II and VII were more commonly observed in patients with EGFR mutation negative. Therefore, we believe that patients with type III or IV are more likely to benefit from targeted therapy. Some research has indicated that GGO and air bronchogram, which are closely related to the lepidic predominant subtype, are significant risk factors of EGFR mutation in the context of solitary lung cancer;[7,22–24,29–31] this may be a good explanation to our results. Considering that most patients with type II and VII do not carry EGFR mutations, standard chemotherapy is still the first-line treatment strategy and targeted therapy can be offered to patients with EGFR mutations. Additionally, our study indicates that, for patients with type VI, the presence of subsolid lesion indicates EGFR mutation, especially when all lesions are subsolid. Recently, multifocal LADC has been increasingly detected in lung cancer screening programs, leading to a strong interest in the field and controversies about the diagnosis and management of these lesions.[14,32] Some scholars believe that surgical resection is the optimal treatment for multifocal LADC;[25] however, because resection of multicentric lesions has some limitations in terms of pulmonary reserve, targeted therapy may provide new therapeutic strategies for multifocal LADC presenting with subsolid lesions.

Some clinical studies have indicated that patients with 19 deletion mutation showed significantly longer progression-free survival and overall survival as compared with patients with L858R mutation, which indicates that tumors with 19 deletion or L858R mutations should be treated differently.[33–35] In the present study, we found that type VII tumors were closely related to 19 deletion mutation positive and non-L858R mutation positive, which may provide more information for the choice of treatment strategy and the prediction of prognosis in patients with LADC.

This study had several limitations that should be considered. First, considering that most patients in our study only received EGFR mutation test, we focused on this most commonly mutated gene of LADC, and future studies on the relationship between CT morphological classification of LADC and other mutant genes are needed.

Second, the sample size of some types was not large enough to draw firm conclusions even though we included a large number of patients with known EGFR mutation statuses. Third, for patients with multifocal lesions, genetic testing could not be carried out on all lesions due to unavailability of histological specimens. We intend to continue to investigate the relationships among EGFR mutation status, CT features, treatment protocols, and survival of patients with multifocal LADC in the future.

Conclusion

In conclusion, our findings demonstrate that LADC can be categorized into eight types based on CT imaging, and this morphological classification is related to the presence of EGFR mutation. These results may contribute to improving the accuracy rate for the diagnosis of LADC, while suggesting the presence of underlying EGFR genetic mutations.

Abbreviations

CT, computed tomography; LADC, lung adenocarcinoma; EGFR, epidermal growth factor receptor; GGO, ground-glass opacity; PACS, picture archiving and communication system; PET/CT, positron emission tomography-computed tomography.

Data Sharing Statement

The datasets during and/or analyzed during the current study available from the corresponding author (Xing-Tao Huang) on reasonable request.

Ethics Approval and Consent to Participate

This study and all its protocols were approved by the ethics committee of our institute, and the need for informed consent was waived due to the retrospective nature.

Funding

This study was supported by Chongqing Scientific & Technological Support Funds (cstc2017jcyjAX0281).

Disclosure

Dr Xing-Tao Huang reports grants from cstc2017jcyjAX0281, during the conduct of the study. The authors declare that they have no other competing interests.

References

1. Siegel RL, Miller KD, Jemal A. Cancer statistics, 2019. *CA Cancer J Clin*. 2019;69:7–34. doi:10.3322/caac.21551
2. Pascoe HM, Knipe HC, Pascoe D, Heinze SB. The many faces of lung adenocarcinoma: a pictorial essay. *J Med Imaging Radiat Oncol*. 2018;62:654–661. doi:10.1111/1754-9485.12779
3. Saito M, Shiraishi K, Kunitoh H, et al. Gene aberrations for precision medicine against lung adenocarcinoma. *Cancer Sci*. 2016;107 (6):713–720. doi:10.1111/cas.12941
4. Jin Y, Shi X, Zhao J, et al. Mechanisms of primary resistance to EGFR targeted therapy in advanced lung adenocarcinomas. *Lung Cancer*. 2018;124:110–116. doi:10.1016/j.lungcan.2018.07.039
5. Rosell R, Carcereny E, Gervais R, et al. Erlotinib versus standard chemotherapy as first-line treatment for European patients with advanced EGFR mutation-positive non-small-cell lung cancer (EURTAC): a multicentre, open-label, randomised Phase 3 trial. *Lancet Oncol*. 2012;13:239–246. doi:10.1016/S1470-2045(11) 70393-X
6. Ciuleanu T, Stelmakh L, Cicenas S, et al. Efficacy and safety of erlotinib versus chemotherapy in second-line treatment of patients with advanced, non-small-cell lung cancer with poor prognosis (TITAN): a randomised multicentre, open-label, phase 3 study. *Lancet Oncol*. 2012;13(3):300–308. doi:10.1016/S1470-2045(11)70385-0
7. Liu Y, Kim J, Qu F, et al. CT features associated with epidermal growth factor receptor mutation status in patients with lung adenocarcinoma. *Radiology*. 2016;280(1):271–280. doi:10.1148/ radiol.2016151455
8. Goldstraw P, Chansky K, Crowley J, et al. The IASLC lung cancer staging project: proposals for revision of the TNM stage groupings in the forthcoming (Eighth) Edition of the TNM classification for lung cancer. *J Thorac Oncol*. 2016;11(1):39–51. doi:10.1016/j.jtho.2015.09.009
9. Travis WD, Brambilla E, Noguchi M, et al. International Association for theStudy of Lung Cancer/American Thoracic Society/European Respiratory Society international multidisciplinary classification of lung adenocarcinoma. *J Thorac Oncol*. 2011;6(2):244–285.
10. Cohen JG, Reymond E, Jankowski A, et al. Lung adenocarcinomas: correlation of computed tomography and pathology findings. *Diagn Interv Imaging*. 2016;97(10):955–963. doi:10.1016/j.diii.2016.06.021
11. Hutchinson BD, Shroff GS, Truong MT, et al. Spectrum of lung adenocarcinoma. *Semin Ultrasound CT MR*. 2019;40(3):255–264. doi:10.1053/j.sult.2018.11.009
12. Moon Y, Lee KY, Park JK. The prognosis of invasive adenocarcinoma presenting as ground-glass opacity on chest computed tomography after sublobar resection. *J Thorac Dis*. 2017;9(10): 3782–3792. doi:10.21037/jtd.2017.09.40
13. Lederlin M, Puderbach M, Muley T, et al. Correlation of radio- and histomorphological pattern of pulmonary adenocarcinoma. *Eur Respir J*. 2013;41(4):943–951. doi:10.1183/09031936.00056612
14. Xue X, Wang P, Xue Q, et al. Comparative study of solitary thin-walled cavity lung cancer with computed tomography and pathological findings. *Lung Cancer*. 2012;78(1):45–50. doi:10.1016/j. lungcan.2012.06.004
15. Tan Y, Gao J, Wu C, et al. CT characteristics and pathologic basis of solitary cystic lung cancer. *Radiology*. 2019;291(2):495–501. doi:10.1148/radiol.2019181598
16. Mansuet-Lupo A, Barritault M, Alifano M, et al. Proposal for a combined histomolecular algorithm to distinguish multiple primary adenocarcinomas from intrapulmonary metastasis in patients with multiple lung tumors. *J Thorac Oncol*. 2019;14(5):844–856. doi:10.1016/j.jtho.2019.01.017
17. Chung JH, Choe G, Jheon S, et al. Epidermal growth factor receptor mutation and pathologic-radiologic correlation between multiple lung nodules with ground-glass opacity differentiates multicentric origin from intrapulmonary spread. *J Thorac Oncol*. 2009;4(12):1490–1495. doi:10.1097/JTO.0b013e3181bc9731

18. Revel MP, Carette MF, Torrent M, et al. Diagnosis and standardized report for non-small cell lung cancer. *Diagn Interv Imaging*. 2014;95(7–8):727–738. doi:10.1016/j.diii.2014.06.007
19. Herrera LS, Fernandez-Fabrellas E, Juan SG, et al. Predicting malignant and paramalignant pleural effusions by combining clinical, radiological and pleural fluid analytical parameters. *Lung*. 2017;195(5):653–660. doi:10.1007/s00408-017-0032-3
20. Yang MF, Tong ZH, Wang Z, et al. Development and validation of the PET-CT score for diagnosis of malignant pleural effusion. *Eur J Nucl Med Mol Imaging*. 2019;46(7):1457–1467. doi:10.1007/s00259-019-04287-7
21. Brun C, Gay P, Cottier M, et al. Comparison of cytology, chest computed and positron emission tomography findings in malignant pleural effusion from lung cancer. *J Thorac Dis*. 2018;10(12):6903–6911. doi:10.21037/jtd.2018.11.127
22. Sabri A, Batool M, Xu Z, et al. Predicting EGFR mutation status in lung cancer: proposal for a scoring model using imaging and demographic characteristics. *Eur Radiol*. 2016;26(11):4141–4147. doi:10.1007/s00330-016-4252-3
23. Zhang H, Cai W, Wang Y, et al. CT and clinical characteristics that predict risk of EGFR mutation in non-small cell lung cancer: a systematic review and meta-analysis. *Int J Clin Oncol*. 2019;24(6):649–659. doi:10.1007/s10147-019-01403-3
24. Hong SJ, Kim TJ, Choi YW, et al. Radiogenomic correlation in lung adenocarcinoma with epidermal growth factor receptor mutations: imaging features and histological subtypes. *Eur Radiol*. 2016;26(10):3660–3668. doi:10.1007/s00330-015-4196-z
25. Chen Y, Yang Y, Ma L, et al. Prediction of EGFR mutations by conventional CT-features in advanced pulmonary adenocarcinoma. *Eur J Radiol*. 2019;112:44–51. doi:10.1016/j.ejrad.2019.01.005
26. Wu S, Shen G, Mao J, et al. CT radiomics in predicting EGFR mutation in non-small cell lung cancer: a Single Institutional Study. *Front Oncol*. 2020;10:542957. doi:10.3389/fonc.2020.542957
27. Tu W, Sun G, Fan L, et al. Radiomics signature: a potential and incremental predictor for EGFR mutation status in NSCLC patients, comparison with CT morphology. *Lung Cancer*. 2019;132:28–35. doi:10.1016/j.lungcan.2019.03.025
28. Jia TY, Xiong JF, Li XY, et al. Identifying EGFR mutations in lung adenocarcinoma by noninvasive imaging using radiomics features and random forest modeling. *Eur Radiol*. 2019;29(9):4742–4750. doi:10.1007/s00330-019-06024-y
29. Wang H, Zhang W, Wang K, et al. Correlation between EML4-ALK, EGFR and clinicopathological features based on IASLC/ATS/ERS classification of lung adenocarcinoma. *Medicine (Baltimore)*. 2018;97(26):e11116. doi:10.1097/MD.0000000000011116
30. Motono N, Funasaki A, Sekimura A, et al. Prognostic value of epidermal growth factor receptor mutations and histologic subtypes with lung adenocarcinoma. *Med Oncol*. 2018;35(3):22. doi:10.1007/s12032-018-1082-y
31. Onoda H, Kimura T, Tao H, et al. Air bronchogram in pleomorphic carcinoma of the lung is associated with favorable prognosis. *Thorac Cancer*. 2018;9(6):718–725. doi:10.1111/1759-7714.12638
32. Guo H, Shen-Tu Y. [Research progress in diagnosis and management strategies of multiple primary lung cancer]. *Zhongguo Fei Ai Za Zhi*. 2016;19(5):307–311. (Chinese). doi:10.3779/j.issn.1009-3419.2016.05.12
33. Yu JY, Yu SF, Wang SH, et al. Clinical outcomes of EGFR-TKI treatment and genetic heterogeneity in lung adenocarcinoma patients with EGFR mutations on exons 19 and 21. *Chin J Cancer*. 2016;35:30. doi:10.1186/s40880-016-0086-2
34. Won YW, Han JY, Lee GK, et al. Comparison of clinical outcome of patients with non-small-cell lung cancer harbouring epidermal growth factor receptor exon 19 or exon 21 mutations. *J Clin Pathol*. 2011;64(11):947–952. doi:10.1136/jclinpath-2011-200169
35. Rosell R, Moran T, Queralt C, et al. Screening for epidermal growth factor receptor mutations in lung cancer. *N Engl J Med*. 2009;361(10):958–967. doi:10.1056/NEJMoa0904554